First-principles calculations on effects of Al and Ga dopants on atomic and electronic structures of amorphous $Ge_2Sb_2Te_5$

Supplementary Material

1. Cell-size test

We generated five Al-doped GST models containing 160 atoms and two Al-doped GST models containing 320 atoms in the same procedure described in the paper. Total RDF and atom-resolved CN are shown in Fig. S1. Overall shape and main features of RDF are similar except the second peak from RDF is slightly shortened. The difference of second peak is attributed to the mid-range to which the band gap and local structures are insensitive. The atom-resolved CNs are also consistent with smaller samples. Band gap from 320-atom models are compared with those from 160-atom models. Band gap energies from 160-atom models and 320-atom models estimated by Tauc plot are 0.49 and 0.50 eV, respectively.

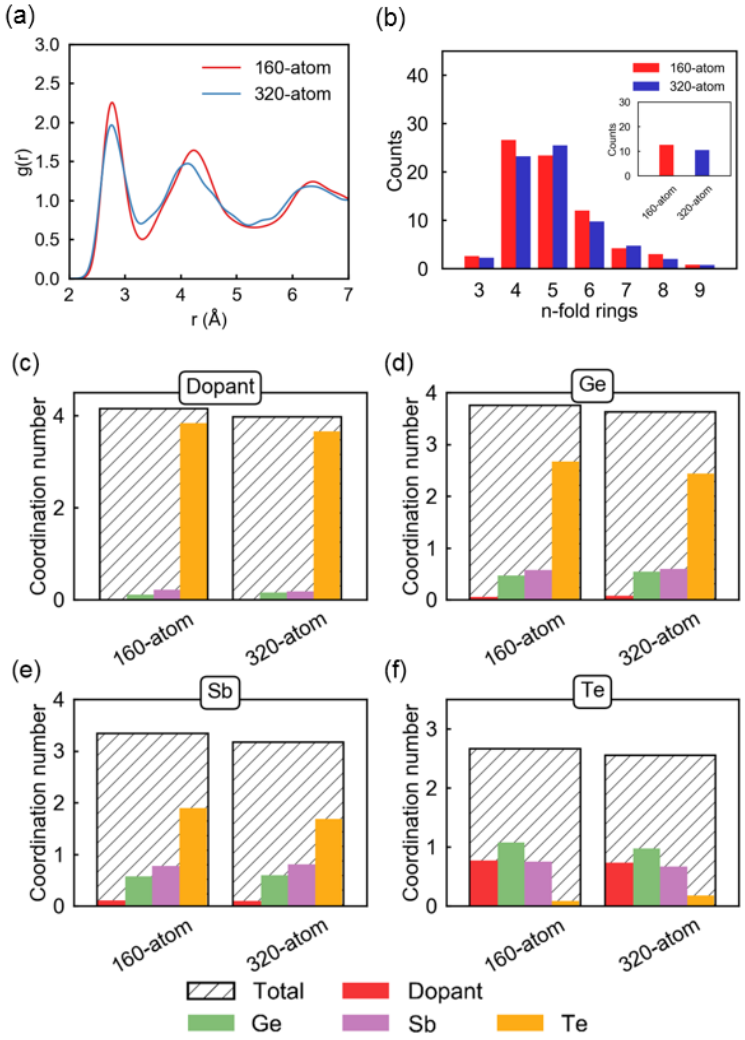

Fig. S1. (a) Total RDF of *a*-GST with 10 at% of Al doping, (b) ring distributions in the given cells, and (c)-(f) atom-resolved CNs around dopant, Ge, Sb, and Te, respectively.

2. Changes of atomic structures and band gap at different doping densities

In order to reproduce the gap trend reported in experiment,[1] five doped *a*-GST models containing 36 Al or Zn atoms (doping concentration of 20 at%) were additionally generated by melt-quench simulations and the average band gap estimated by Tauc plot are plotted in Fig. S2. The values for each data point are tabulated in Table SI and SII. The solid lines and dotted line in the figure represent the linear regression for the calculated and the experimental band gap, respectively. The slopes of the fitted lines for Al and Zn doping are 0.0053 and 0.0051 eV/at%, respectively, and the slope for experimental data is 0.0042 eV/at%. Therefore, the trend of increasing band gap upon metal doping is well reproduced in the calculation.

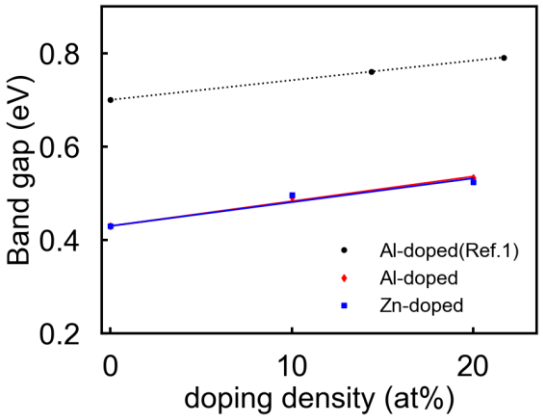

Fig. S2. The calculated band gap and measured band gap are plotted by solid lines and dotted lines, respectively.

Table SI. Calculated band gap (all values are in eV.)

Doping density (at%)	0	10	20
Al-doped GST	0.43	0.49	0.53
Zn-doped GST	0.43	0.50	0.52

Table SII. Measured band gap (all values are in eV.)

Doping density (at%)	0	14.4	21.7
Al-doped GST[1]	0.70	0.76	0.79

In the total RDF shown in Fig. S3, it is seen that the doping mostly changes the short-range order rather than the mid-range order, which implies that the given band gap changes are originated from the local environment variation from the doping. To provide clear insights into reasons for band gap increase, we evaluate the number density of the MTe_4 units in the doped GST as the doping concentration increases from 10 at% to 20 at%. The number density of $AlTe_4$ ($ZnTe_4$) units increases from 1.7/nm^3 (1.9/nm^3) to 2.6/nm^3 (3.0/nm^3) as the doping concentration increases from 10 at% to 20 at%. The doped a-GST can be considered as a mixture

phase of the MTe_4 units and the host atoms of GST, in which the band gap is widened as the number of MTe_4 units increases.

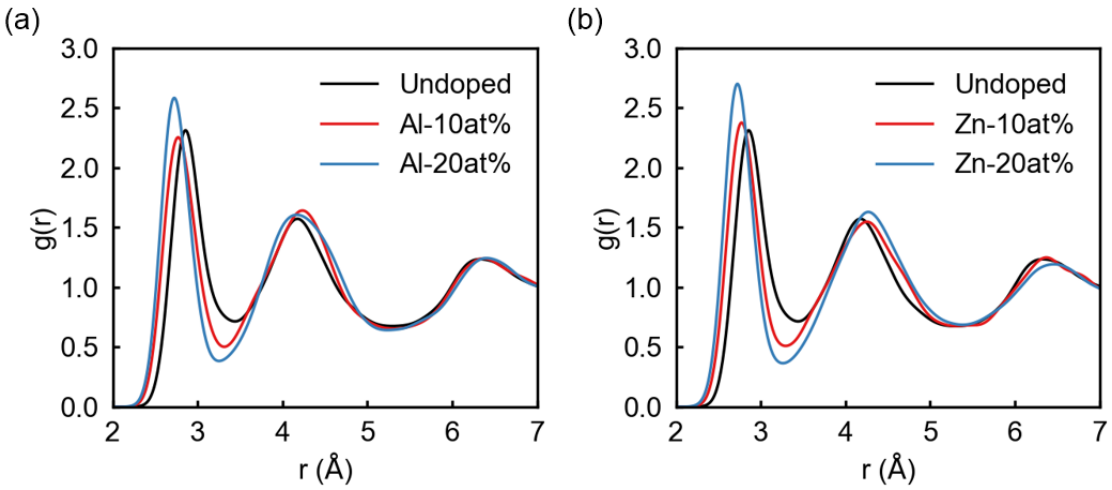

Fig. S3. Total RDF of 0, 10, and 20 at% of Al- and Zn-doped *a*-GST

3. Complex refractive index

We calculated the complex refractive index of undoped and doped *a*-GST and compare the results with the experiment as shown in Fig. S4 (a). In low photon energy (below 0.5 eV), the calculated refractive index of undoped *a*-GST is 5.4 and those of doped *a*-GST are 4.9, 4.7, and 4.9 for Al, Zn, and Ga, respectively. (The experimental values for undoped *a*-GST range from 3.3 to 4.5.[3,4]) We also present the extinction coefficient (*k*) in the Fig. S4 (b), and the experimental value for Al-doped GST[2] is compared with calculated result (Fig. S4 (c)). It is found that the *k* of doped *a*-GST shows similar curves regardless of dopants. Fig. S4 (c) shows that the changes in the calculated extinction coefficients by Al doping are qualitatively matched to results from experiment in which the doping lowers the *k* of *a*-GST. The calculated *n* and *k* are overestimated because of the underestimation of band gap in PBE, but the trend upon metal doping is turned out to be valid. We note that both *n* and *k* decrease upon metal doping, which is a result of the band gap increase in doped *a*-GST.

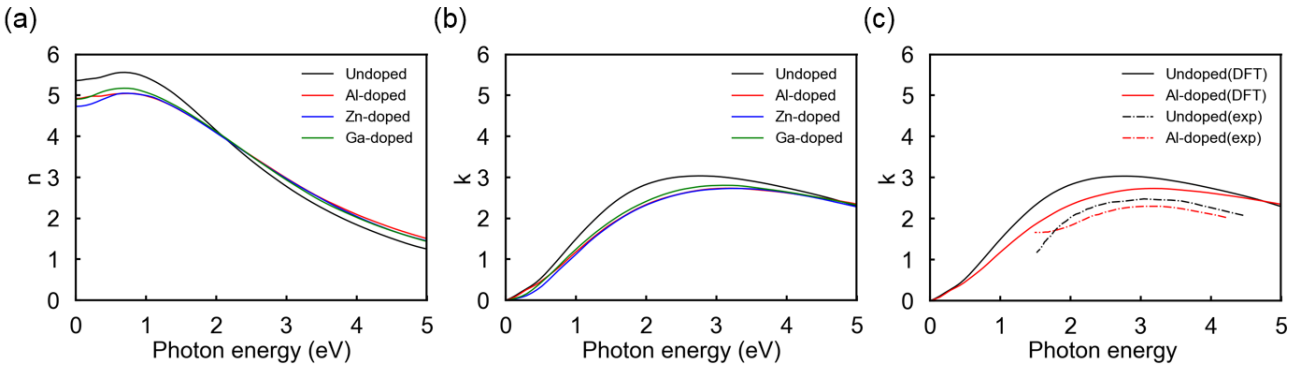

Fig. S4. (a) Refractive index and (b) extinction coefficient of doped a-GST are shown. Extinction coefficients from DFT calculations are compared with experimental results in (c).

4. References

[1]G. Wang *et al.*, J. Phys. D: Appl. Phys. **45**, 375302 (2012).
[2]S. Wei *et al.*, *Opt. Express* **15**, 10584 (2007).
[3]W. H. P. Pernice and H. Bhaskaran, *Appl. Phys. Lett.* **101**, 171101 (2012).
[4]Z. Xu *et al.*, *RSC Adv.* **8**, 21040 (2018).